

# **A Self-activation Strategy to Prepare ZIF-8 Derived N, O Co-doped Meso-microporous Carbon for Zinc Ion Hybrid Capacitors**

Yanyan Wang<sup>a</sup>, Te Huo<sup>a</sup>, Chunxia Chen<sup>a</sup>, Lan Wang<sup>b\*</sup>, Lichao Tan<sup>c</sup>, Xiaoliang Wu<sup>a, c\*</sup>, Xin  
Wang<sup>c\*</sup>

<sup>a</sup> Center for Innovative Research in Synthetic Chemistry and Resource Utilization, College of  
Chemistry, Chemical Engineering and Resource Utilization, Northeast Forestry University, 26  
Hexing Road, Harbin 150040, PR China

<sup>b</sup> School of New Energy, Ningbo University of Technology, Ningbo 315336, Zhejiang, China

<sup>c</sup> Wanli Energy Technology Development Co., Ltd, Zhejiang Wanli University, Ningbo, 315100,  
China

\*Address correspondence to: [Wanglan@nbut.edu.cn](mailto:Wanglan@nbut.edu.cn) (L. Wang), [wuxiaoliang90@163.com](mailto:wuxiaoliang90@163.com) (X.L.  
Wu), [wangx@zwu.edu.cn](mailto:wangx@zwu.edu.cn) (X. Wang)

## 1. Experimental section

### 1.1. Materials characterization

Powder X-ray diffractometer (XRD) was carried out to determine crystalline structure of the samples. The morphologies were characterized by a scanning electron microscope (SEM JEOL JSM-7500F) and a transmission electron microscope (TEM JEM2010). The chemical elements of samples were analyzed by X-ray photoelectron spectroscopy (ThermoScientific Nexsa). The Brunauer-Emmett-Teller (BET) surface area were determined by nitrogen adsorption/desorption isotherms (BELSORP-MAX) at 77 K. The pore size distribution was analyzed by the Non-Local Density Functional Theory (NLDFT).

### 1.2. Electrochemical measurements

Supercapacitors (SCs). The ZPC-x electrodes were prepared by mixing ZPC-x powders with carbon black, PTFE at a weight ratio of 7:2:1 in absolute alcohol to form a uniformly dispersed slurry. The slurry was then coated onto the nickel foam (1 cm × 1 cm), followed by drying at 60 °C for 12 h. The total mass loading of each electrode was about 3.0 mg. All electrochemical properties of the ZPC-x electrode were evaluated using a three-electrode configuration on a CHI660E electrochemical workstation (Shanghai CH Instrument, China) at room temperature. In the three-electrode device, the Hg/HgO electrode, Pt foil, and 6 M KOH were used as reference electrode, counter electrode, and electrolyte, respectively. The gravimetric specific capacitance ( $C$ , F g<sup>-1</sup>), energy density ( $E$ , Wh kg<sup>-1</sup>), and power density ( $P$ , W kg<sup>-1</sup>) were calculated based on the mass of the active materials (porous carbon) in electrode using the equations as follows.

$$C = (I\Delta t)/(m\Delta V)$$

Where  $I$  refers to the discharge current (A),  $\Delta t$  is the discharge time (s),  $m$  is the mass of active materials (g), and  $\Delta V$  is the potential window (V).

Aqueous symmetric supercapacitors. The preparation method for ZPC-x electrodes was identical to that of the SC electrodes as described earlier. Electrochemical measurements including cyclic voltammogram (CV) curves, electrochemical impedance spectroscopy (EIS), galvanostatic charging-discharging (GCD) curves and the long-term cycle were conducted using a CHI660E electrochemical workstation (Shanghai CH Instrument, China) at room temperature. But for the aqueous symmetric supercapacitors, these measurements were carried out in a two-electrode cell with 1 M  $\text{Na}_2\text{SO}_4$  aqueous electrolyte. In the two-electrode setup, two electrodes of the same mass were used as positive and negative electrodes, respectively, and they were separated by a separator. The discharge capacitance of materials ( $C_m$ ,  $\text{F g}^{-1}$ ) of both electrodes, energy density ( $E$ ,  $\text{Wh kg}^{-1}$ ), and power density ( $P$ ,  $\text{W kg}^{-1}$ ) of the device were calculated by the equations as follows.

$$C_m = 4C_s = (2I\Delta t)/(m\Delta V)$$

$$E = C_s(\Delta V)^2/7.2$$

$$P = 3600E/\Delta t$$

Where  $I$  represents the discharge current (A),  $\Delta t$  is the discharge time (s),  $m$  is the mass of active material on each electrode (g),  $\Delta V$  is the potential difference (V), and  $C_s$  is the specific capacitance of the capacitor ( $C_m/4$ ,  $\text{F g}^{-1}$ ).

Zinc ion hybrid capacitors (ZIHCs). The ZPC-x cathode electrodes were prepared by mixing ZPC-x powders with carbon black and PTFE at a weight ratio of 8:1:1 in absolute alcohol to form a uniformly dispersed slurry. The slurry was then coated onto a stainless-steel mesh (D 1.2cm), followed by drying at 60 °C for 12 h. The total mass loading of the electrode was 1.05 to 1.56 mg.

The electrochemical performance of ZPC-x electrodes was tested by a CR2032 type coin cell configuration. ZPC-x samples were served as the cathode, while zinc foil with a thickness of 0.1 mm was employed as the anode. A separator made from glass-fiber paper (GF/F, Whatman) was inserted between the cathode and anode, and a 2 M ZnSO<sub>4</sub> solution was utilized as the electrolyte. GCD curves, rate performance, and the long-term cycle were carried out using the Neware battery testing system. CV curves and EIS spectrum were acquired using CHI660E electrochemical workstation. Specifically, the EIS spectrum was recorded at the open circuit potential (OCP), spanning a frequency range from 100,000 Hz to 0.01 Hz with an amplitude of 5 mV. The specific capacity (C, mAh·g<sup>-1</sup>) based on the mass of the active materials in cathode was directly read from the instrument. The energy density (E, Wh kg<sup>-1</sup>) and the power density (P, W kg<sup>-1</sup>) of ZIHCs were calculated by the equations as follows.

$$E = C(\Delta V)^2/7.2$$

$$P = 3600E/\Delta t$$

Where C is the specific capacity (F g<sup>-1</sup>),  $\Delta V$  is the voltage window (V), and  $\Delta t$  is the discharge time (s).

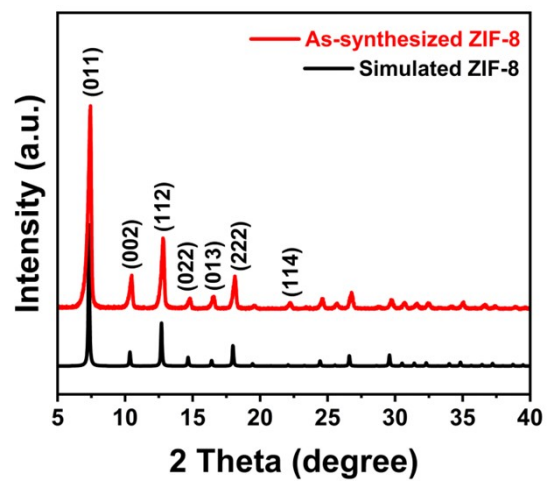


Fig. S1. XRD pattern of ZIF-8.

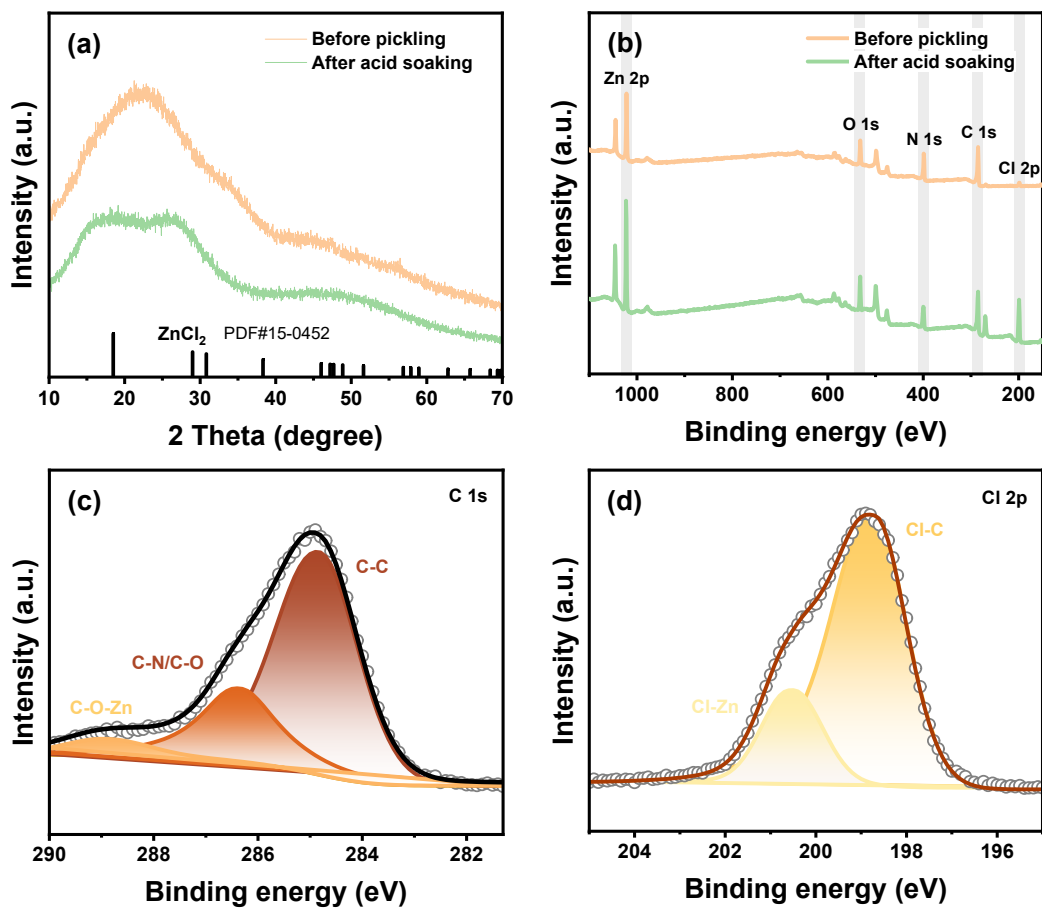


Fig. S2. (a) XRD patterns, and (b) XPS patterns of ZIF-8 after the first pyrolysis before/after acid soaking. (c) C 1s, and (d) Cl 2p high-resolution XPS spectrum of ZIF-8 after the first pyrolysis after acid soaking.

Fig. S3. (a, b) SEM images of ZPC-700.

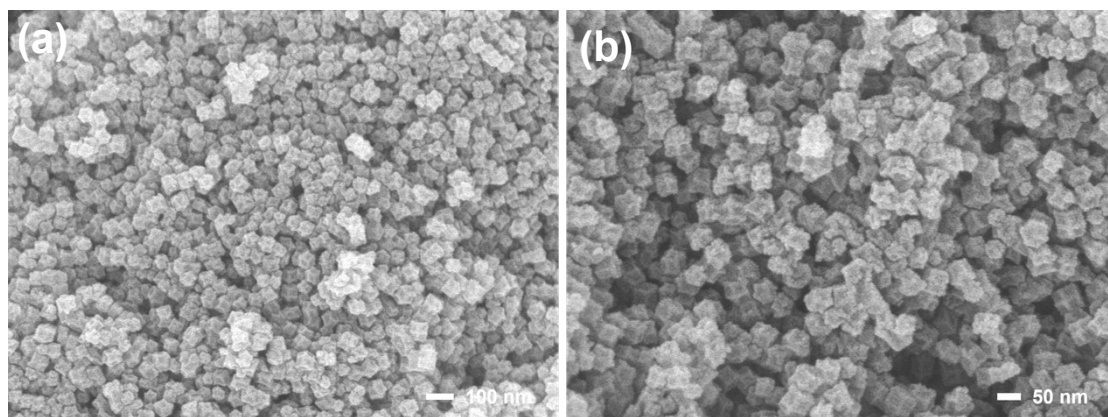


Fig. S4. (a, b) SEM images of ZPC-900.



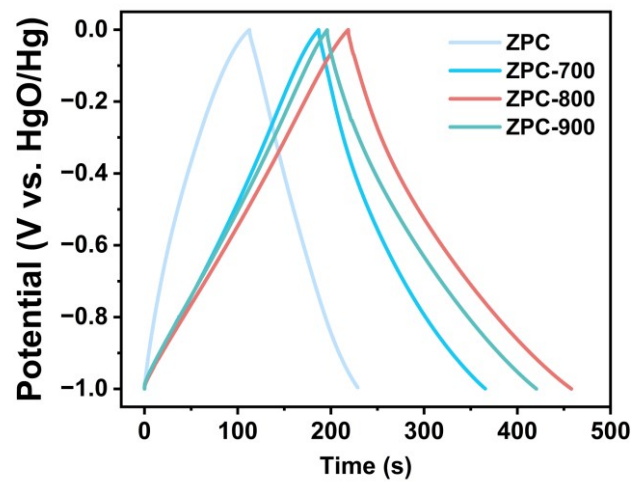


Fig. S5. GCD curves of ZPC, ZPC-700, ZPC-800, and ZPC-900 at  $1.0 \text{ A g}^{-1}$ .

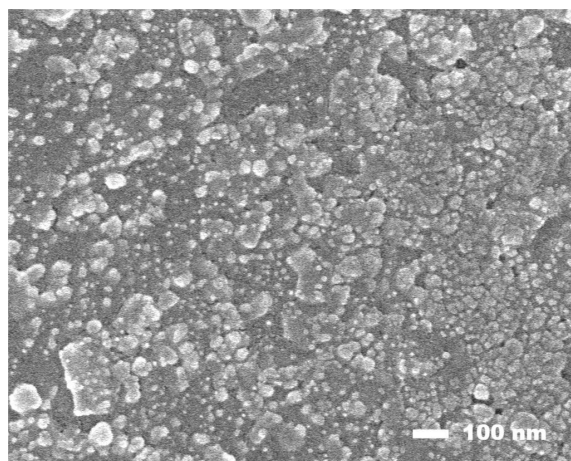


Fig. S6. SEM image of ZPC-800 after 10,000 charge/discharge cycles in three-electrode system.

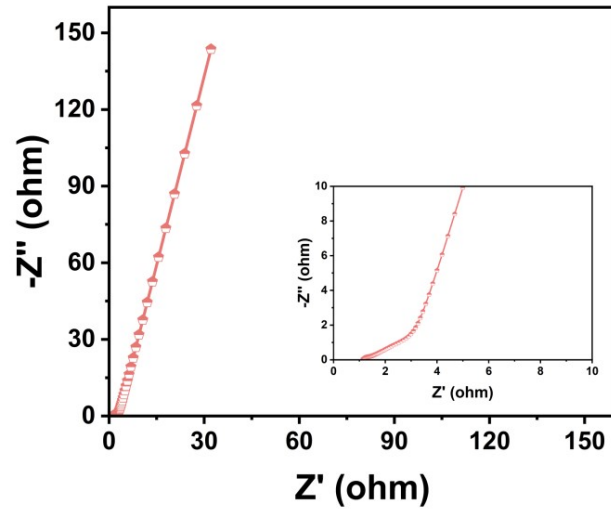


Fig. S7. Nyquist plot of the ZPC-800//ZPC-800 symmetric supercapacitor.

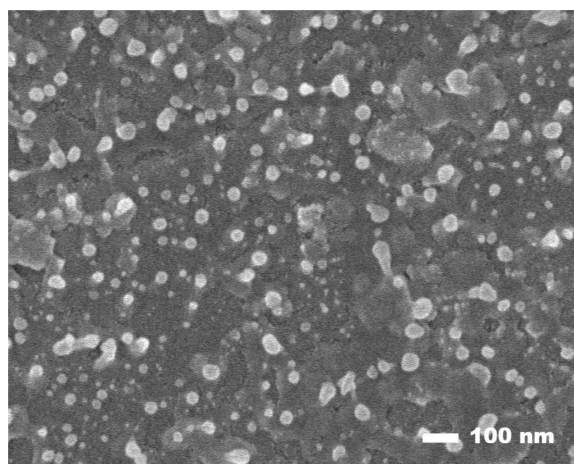


Fig. S8. SEM image of ZPC-800 cathode after 10,000 charge/discharge cycles in ZIHCs.

Fig. S9. The linear fitting of log (specific current) against log (scan rate) at redox peaks of (a) ZPC, (c) ZPC-700, and (e) ZPC-900. The capacitive and diffusion contribution ratios to the total capacity at different scan rates of (b) ZPC, (d) ZPC-700, and (f) ZPC-900.

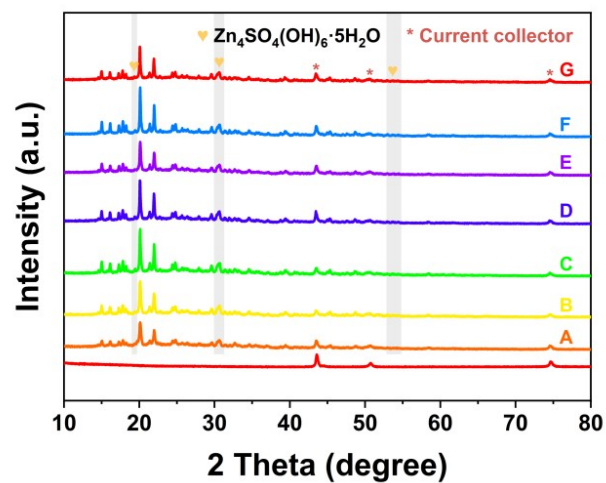


Fig. S10. Ex situ XRD patterns of current collector and the selected voltage states of ZPC-800.